

Pyrrole-Appended Derivatives of *O*-Confused Oxaporphyrins and Their Complexes with Nickel(II), Palladium(II), and Silver(III)

Miłosz Pawlicki and Lechosław Latos-Grażyński*^[a]

Abstract: Condensation of 2,4-bis(phenylhydroxymethyl)furan with pyrrole and *p*-toluylaldehyde formed, instead of the expected 5,20-diphenyl-10,15-di(*p*-tolyl)-2-oxa-21-carbaporphyrin, a pyrrole addition product [(H,pyr)-OCPH]₂; this product can formally be considered as an effect of hydrogenation of 3-(2'-pyrrolyl)-5,20-diphenyl-10,15-di(*p*-tolyl)-2-oxa-21-carbaporphyrin [(pyr)OCPH]H). The new oxacarporphyrinoid presents the ¹H NMR spectroscopy features of an aromatic molecule, including the upfield shift of the inner H21 atom. Insertion of NiCl₂ or PdCl₂ into [(H,pyr)OCPH]₂ gave two structurally related organometallic complexes, [(pyr)OCP]Ni^{II} and [(pyr)OCP]Pd^{II}, in which the metal ions are bound by three pyrrolic nitrogens and the trigonally hybridized C21 atom of the inverted furan. The reaction of [(H,pyr)OCPH]₂ with silver(I) acetate

yields a stable Ag^{III} complex [(C₂H₅O,pyr)OCP]Ag^{III} substituted at the C3 position by the ethoxy and pyrrole moieties. The macrocyclic frame of [(H,pyr)OCPH]₂ is conserved. Addition of trifluoroacetic acid to [(C₂H₅O,pyr)OCP]Ag^{III} yielded a new aromatic complex [(pyr)OCP]Ag^{III}⁺. The structures of [(pyr)OCP]Ni^{II} and [(C₂H₅O,pyr)OCP]Ag^{III} have been determined by X-ray crystallography. In both molecules the macrocycles are only slightly distorted from planarity and the nickel(II) and silver(III) are located in the NNNC plane. The dihedral angle between the macrocyclic and appended-pyrrole planes of [(pyr)OCP]Ni^{II} reflects the biphenyl-like arrangement

with the NH group pointing out toward the adjacent phenyl ring on the C5 position. Tetrahedral geometry around the C3 atom was detected for [(C₂H₅O,pyr)OCP]Ag^{III}. The Ni–C and Ag–C bond lengths are similar to other nickel(II) or silver(III) carbaporphyrinoids where the trigonal carbon atom coordinates the metal ion. The trend detected in the ¹³C chemical shifts for the appended-pyrrole resonances has been rationalized by the extent of effective conjugation between the macrocycle and the appended pyrrole moiety controlled by the hybridization of the C3 atom and the metal ion oxidation state. The dianionic or trianionic macrocyclic core of the pyrrole-appended derivatives is favored to match the oxidation state of nickel(II), palladium(II), or silver(III), respectively.

Keywords: macrocyclic ligands • nickel • palladium • porphyrinoids • silver

Introduction

The inverted porphyrin 5,10,15,20-tetraaryl-2-aza-21-carbaporphyrin ((CTPPH)H₂)^[1, 2] and its derivatives have revealed a remarkable tendency to stabilize peculiar organometallic compounds containing diamagnetic nickel(II),^[1, 3–6] paramagnetic nickel(II) with one or two Ni–C bonds,^[7, 8] nickel(III),^[9] copper(II),^[10] palladium(II),^[11] antimony(V),^[12] silver(III),^[13] manganese(II) and manganese(III),^[14, 15] zinc(II),^[10, 16] iron(II),^[17, 18] and rhodium(I).^[19]

The ability of carbaporphyrinoids to coordinate metal ions and form metal–carbon bonds^[20] extends beyond the family of inverted porphyrins.^[21–25] In this respect, studies on the

coordination properties of derivatives of *meta*-benzporphyrin, the first synthesized carbaporphyrinoid containing a carbocyclic ring, are of particular significance. Originally the benzene ring was embedded in an octaalkylporphyrin-like environment to give 8,19-dimethyl-9,13,14,18-tetraethyl-*m*-benzporphyrin.^[26] The related macrocycle 6,11,16,21-tetra-phenylbenzporphyrin ((TPmBPH)H) can give organometallic complexes with palladium(II) and platinum(II), [(TPmBP)Pd^{II}] and [(TPmBP)Pt^{II}].^[22] The metal ion is bound in the macrocyclic cavity by three pyrrolic nitrogen atoms and a trigonal carbon atom of the benzene ring. A hydroxy derivative of 8,9,13,14,18,19-hexaalkylbenzporphyrin, that is, 8,19-dimethyl-9,13,14,18-tetraethoxybenzporphyrin ((OBPH)H₂),^[27] coordinates palladium(II) to form the four-coordinate anionic complex [(OBP)Pd^{II}][−] with retention of macrocyclic aromaticity and coordination through a carbon σ donor.^[23] Subsequently the palladium(II) complexes of core-modified oxybenzporphyrin,^[25] nickel(II) and palladium(II)

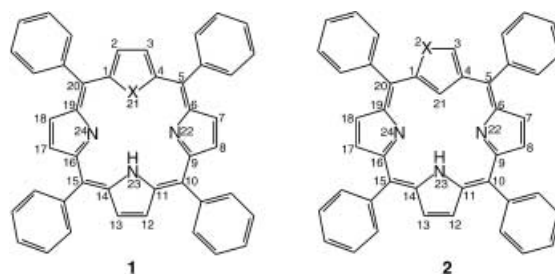
[a] Prof. Dr. L. Latos-Grażyński, M. Pawlicki
Department of Chemistry
University of Wrocław
ul. F. Joliot-Curie 14, 50-383 Wrocław (Poland)
E-mail: LLG@wchuw.chem.uni.wroc.pl

azuliporphyrins,^[28] and silver(III) benzocarboxporphyrin have been investigated.^[29]

Abstract in Polish: W wyniku kondensacji 2,4-bis(fenylohydroksymetylo)furanu z pirolem i aldehydem *p*-toluolowym otrzymano produkt addycji pirolu do 5,20-difenylo-10,15-di(*p*-toluilo)-2-oksa-21-karbaporfiryny [(H)OCPH]H z wydajnością 10%. Uzyskany makrocykl jest formalnie efektem uwodornienia 3-(2'-pirolilo)-5,20-difenylo-10,15-di-*p*-toluilo-2-oksa-21-karbaporfiryny [(pyr)OCPH]H. Nowy ligand, należący do klasy karbaporfirynoidów, wykazuje właściwości typowe dla związków aromatycznych, w tym górnopolowe przesunięcie wewnętrznego atomu wodoru H21 w widmie ¹H NMR (-5.11 ppm). Insercja niklu bądź palladu do [(H,pyr)OCPH]H₂ daje strukturalnie podobne związki metaloorganiczne: [(pyr)OCP]Ni^{II} i [(pyr)OCP]Pd^{II}, w których jon metalu jest związany przez trzy pirolowe atomy azotu i trygonalny atom węgla C21, pochodzący z odwróconego furanu. Koordynacja wymaga odwodornienia połączonego ze zmianą hybrydyzacji atomu C3 z tetraedrycznej na trygonalną. Struktura tak otrzymanego liganda odpowiada budową "prawdziwej" oksakarboxporfirynie z zachowanym pierścieniem furanowym, podstawionym w pozycji C3 pirolem, [(pyr)OCPH]H. Reakcja [(H,pyr)OCPH]H₂ z octanem srebra daje stabilny kompleks srebra(III) [(C₂H₅O,pyr)OCP]Ag^{III} podstawiony w pozycji C3 grupą etoksylogą i pirolem. W tym przypadku zachowany jest szkielet wyjściowego makrocyklu, [(H,pyr)OCPH]H₂. Dowodem na koordynację srebra przez atomy azotu jest, widoczne na części sygnałów β-pirolowych rozszczepienie, świadczące o skalarzym sprzężeniu ze srebrem (^{107/109}Ag). Dodanie TFA do [(C₂H₅O,pyr)OCP]Ag^{III} daje nowy, aromatyczny kompleks, [(pyr)OCP]Ag^{III}+ powstały w wyniku eliminacji grupy etoksylogowej. Reakcja ta jest odwracalna. W jej trakcie zachodzi zmiana geometrii wokół węgla C3 z tetraedrycznej na trygonalną, a zmiany struktury elektronowej mają wpływ na cały makrocykl. Dla [(pyr)OCP]Ni^{II} i [(C₂H₅O,pyr)OCP]Ag^{III} otrzymano struktury krystaliczne. W obu przypadkach planarność makrocyklu jest tylko nieznacznie zaburzona, a nikiel(II) i srebro(III) znajdują się w płaszczyźnie NNNC. Kąt dwusieczny pomiędzy płaszczyzną makrocyklu a dołączonym pirolem w [(pyr)OCP]Ni^{II} zbliżony jest do wartości charakterystycznej dla bifenyli i wynosi 26.4° z grupą NH skierowaną w stronę pobliskiego pierścienia 5-fenylowego. Stwierdzono tetraedryczną geometrię wokół atomu C3 w [(C₂H₅O,pyr)OCP]Ag^{III}. Otrzymane długości wiązań, odpowiednio Ni–C (1.892(4) Å) i Ag–C (2.020(7) Å) są zgodne z innymi przykładami niklu(II) bądź srebra(III), związanego przez karbaporfirynoid, który koordynuje przez trygonalny atom węgla. Zmiany przesunięć chemicznych ¹³C NMR, zaobserwowane dla linii rezonansowych dołączonego pirolu, wynikają z rozszerzenia delokalizacji makrocyklicznej na dodatkowy pierścień heterocykliczny, a kontrolowanej zmianą hybrydyzacji atomu C3 i stopniem utlenienia jonu metalu. Dwu- bądź trójwymiarowy charakter centrum koordynacji badanego liganda odpowiada za preferencje w wiązaniu jonów metali na różnych stopniach utlenienia, odpowiednio niklu(II), palladu(II) i srebra(III).

Pursuing our interest in benziporphyrin coordination chemistry, we have recently reported on 5,10,15,20-tetraphenyl-*p*-benzporphyrin ((TPpBPH)H)—isomeric to 6,11,16,21-tetraphenyl-*m*-benzporphyrin—with the benzene ring linked at the *para* positions.^[24] Significantly this *p*-benzporphyrin forms a complex with cadmium(II) and reveals an unprecedented η² Cd^{II}–arene interaction.

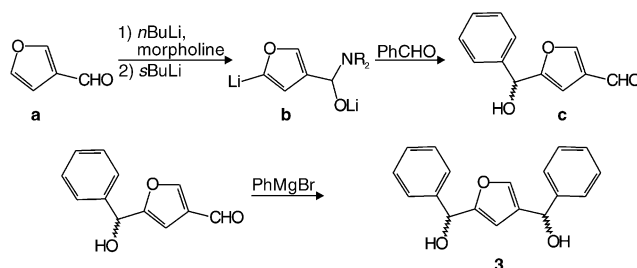
In the present work we describe the synthesis and reactivity of a new carbaporphyrinoid. The molecule has been constructed by applying the heteroatom confusion concept (Scheme 1). Thus, by interchanging a heteroatom with a β-methine group of the same five-membered ring one can transform 5,10,15,20-tetraphenyl-21-heteroporphyrin (**1**) into 5,10,15,20-tetraphenyl-2-hetero-21-carbaporphyrin (**2**), which, while porphyrin-like in character, is expected to have fundamentally different electronic and coordination properties. Previously we probed such an approach to obtain 5,10,15,20-tetraphenyl-2-thia-21-carbaporphyrin.^[30, 31] Here the synthesis of *O*-confused 5,10,15,20-tetraphenyl-21-oxaporphyrin derivatives and their ability to coordinate nickel(II), palladium(II), and silver(III) are explored.



Scheme 1. The heteroatom confusion concept.

Results and Discussion

Synthesis of the oxacarboxporphyrins: The key step in the synthesis of 5,10,15,20-tetraaryl-2-oxa-21-carboxporphyrins is the construction of the condensation precursor, that is, 2,4-bis(phenylhydroxymethyl)furan (**3**; Scheme 2), which is a

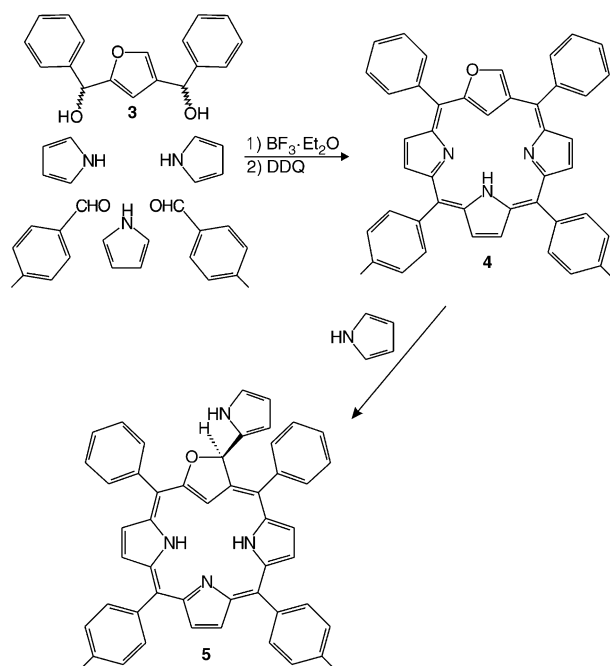


Scheme 2. Synthesis of the condensation precursor 2,4-bis(phenylhydroxymethyl)furan (**3**).

suitable synthon for introducing the inverted furan ring into a porphyrin-like skeleton. The lithiation of an α-amino alkoxide, derived from 3-furancarboxaldehyde **a** was predominantly directed to a remote α site of the furan ring by using

“blocking” amine components—morpholine and *sec*-butyllithium.^[32] The formed 2-furyllithium derivative **b**, when treated with benzaldehyde, yielded 2-(phenylhydroxymethyl)-4-furancarboxaldehyde **c**. The reaction with a phenyl Grignard reagent was applied to convert this aldehyde into the targeted compound **3**.

The procedure applied to synthesize the 5,10,15,20-tetraaryl-2-oxa-21-carbaporphyrin followed the methodology previously utilized for the synthesis of heteroporphyrins^[33] including 5,10,15,20-tetraphenyl-2-thia-21-carbaporphyrin.^[30] Thus, condensation of **3** with pyrrole and *p*-toluylaldehyde (1:3:2 molar ratio) in a one-pot, two-step synthesis at room temperature was expected to yield 5,20-diphenyl-10,15-di(*p*-tolyl)-2-oxa-21-carbaporphyrin (**4**; Scheme 3). However, contrary to expectations, the condensation did not stop at the

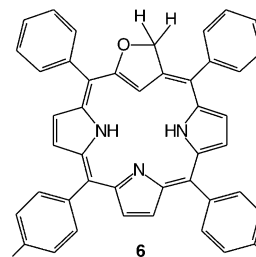


Scheme 3. Condensation of **3** with pyrrole and *p*-toluylaldehyde. The condensation does not stop at the expected oxacarporphyrin **4** and the pyrrole addition product **5** is formed. DDO = 2,3-dichloro-5,6-dicyano-1,4-benzoquinone.

putative **4** and the pyrrole addition product **5** was obtained in a relatively high yield of approximately 10%. An attempt was made to direct the process of formation of the 2-oxa-21-carbaporphyrin, based on the presumption that a substoichiometric concentration of pyrrole would favor the formation of **4**. However, several attempted condensations with various pyrrole concentrations led to the isolation of **5** as the single 2-oxa-21-carbaporphyrin related product. It is worth mentioning that an aza analogue of **5**, 2-aza-3-(2'-pyrrolyl)-5,10,15,20-tetraphenyl-21-carbaporphyrin, which is considered as the isomer of tetraphenylsapphyrin, was reported as a product in the Rothmund condensation.^[34] The identity of **5** has been confirmed by a combination of NMR spectroscopy, including NOESY, HMQC, and HMBC experiments, and high-resolution mass spectrometry.

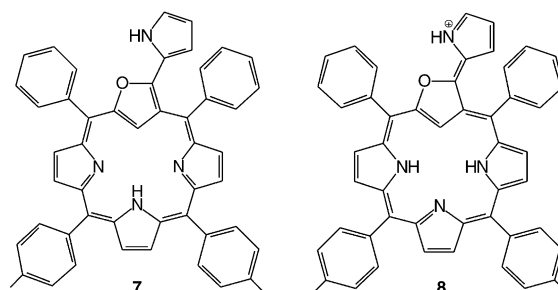
Two different pathways may lead to formation of **5**. The first involves an addition of pyrrole to preformed *O*-confused 2-oxa-21-carbaporphyrin **4**. Alternatively, attack of pyrrole could take place on the furan either at the precursor or at the porphyrinogen stage.

The isolated carbaporphyrinoid **5** is structurally related to the hypothetical 3,3-dihydro-5,20-diphenyl-10,15-di(*p*-tolyl)-2-oxa-21-carbaporphyrin (**6**; Scheme 4) as both contain an identical macrocyclic frame. In the same line of consideration, macrocycles **4** and **6** are mutually interconvertible by a hydrogenation/dehydrogenation step if the addition of the two hydrogen atoms is localized on the C3 position and one of the internal nitrogen atoms.



Scheme 4. Hypothetical 3,3-dihydro-5,20-diphenyl-10,15-di(*p*-tolyl)-2-oxa-21-carbaporphyrin (**6**) which is structurally related to the isolated carbaporphyrinoid **5**.

Studies on the coordination chemistry of **5** (see below) revealed that the coordination implies transformation into the novel structural form **7** (Scheme 5). The macrocycle **7** has not been detected directly, but the related structure has been trapped after the insertion of the metal ions. It is important to



Scheme 5. Structurally related macrocycles **7** and **8**.

note that, formally, **7** can be created from the tetraarylporphyrin by replacement of the pyrrolic fragment with 2-(2'-furyl)pyrrole, that is, by a moiety, which may provide an external conjugation route. The structures **5** and **7** are mutually interconvertible by hydrogenation/dehydrogenation in the same way as already described for the **4** and **6** couple.

From now on we will use the symbol *OCP* to denote the hypothetical dianion obtained from the *O*-confused oxaporphyrin by abstraction of a pyrrolic NH proton and the proton attached at C21. The atoms or groups attached to the C3 atom will be indicated by a prefix enclosed in parentheses. The group attached at C21 will appear as a suffix. A similar description will be used for the hypothetical trianion **6**, formally a dihydrogenation product of **4**. Consequently the

following acronyms correspond to the neutral structures already discussed: **4**: [(H)OCPh]H; **5**: [(H,pyr)OCPh]H₂; **6**: [(H,H)OCPh]H₂; **7**: [(pyr)OCPh]H.

Spectroscopic characterization of 5: The electronic absorption spectra of **5** demonstrate the Soret band (437 nm) accompanied by a set of four Q bands (Figure 1). The spectroscopic pattern is typical for aromatic carbaporphyrinoids. The

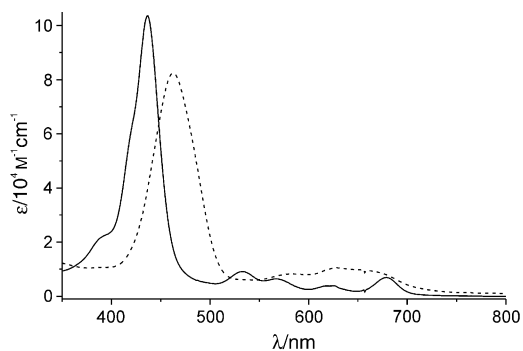


Figure 1. The electronic absorption spectra of **5** (solid line) and (**5-H**)⁺ in dichloromethane.

isosbestic points, corresponding to a single protonation step, were detected in the course of titration of a dichloromethane solution of **5** with trifluoroacetic acid (TFA) to produce the monocationic form (**5-H**)⁺. A strong bathochromic shift of the Soret band to 463 nm was observed for (**5-H**)⁺. Acid titration is accompanied by a distinct color change from brown to green.

The complete assignment of all resonances in the ¹H NMR spectrum for **5** (Figure 2) was obtained by means of 2D ¹H NMR COSY and NOESY experiments, with the unique NOE correlation between H3 and the *ortho* protons of the phenyl group attached to C5 as a starting point. All pyrrole resonances ($\delta = 8.49$ (H17), 8.44 (H18; AB, ³J = 4.9 Hz), 8.47 (H12), 8.45 (H13; AB, ³J = 4.6 Hz), 8.47 (H8), 8.29 (H7; AB, ³J = 4.9 Hz) ppm) are shifted downfield due to the ring-current effect. The peculiar position of the methine H3 resonance at 8.09 ppm was noted. The hydrogen atom is bound to a tetrahedral carbon atom, but the strong downfield shift of its signal is caused by a combination of two effects: the substitution by the oxygen atom at the 2-position and the deshielding contribution of the ring-current effect. At the same time the ¹³C NMR chemical shift for C3 ($\delta = 85.3$ ppm) is consistent with tetrahedral hybridization. Essentially, molecule **5** demonstrates the aromaticity due for the typical 18 π electron delocalization pathway (Scheme 3). The strongly upfield positions of the H21 ($\delta = -5.11$ ppm) and inner proton ($\delta = -2.47, -2.79$ ppm at 188 K) resonances and the significant chemical shift difference ($\Delta\delta = 9.52$ ppm) between the inner NH and the appended-pyrrole NH are readily accounted for by the ring-current effect.

A ¹H NMR spectroscopic titration with TFA carried out in CD₂Cl₂ at 228 K demonstrated that addition of a proton resulted in a separate set of resonances that could be assigned directly to (**5-H**)⁺. Protonation takes place at the nitrogen

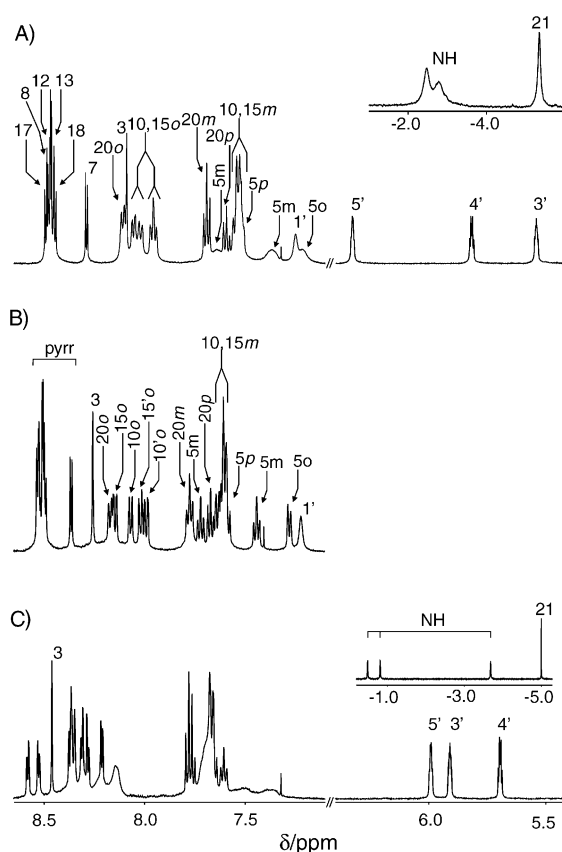
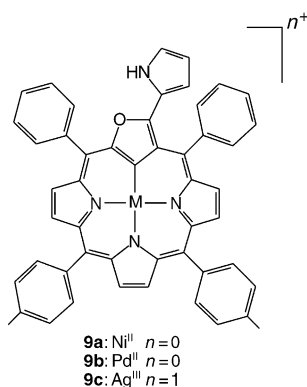


Figure 2. ¹H NMR spectra of: A) **5** (CD₂Cl₂, 298 K), B) **5** (CD₂Cl₂, 253 K), and C) (**5-H**)⁺ (TFA/CD₂Cl₂ (1:5 v/v), 298 K). The insets (not to scale) show the NH and H21 resonances. Peak labels follow systematic position numbering of the macrocycle or denote proton groups. *o*, *m*, and *p* = the *ortho*, *meta*, and *para* positions of *meso*-phenyl (Ph) or *meso-p*-tolyl (Tol) rings, respectively.

atoms, as documented by the rise of three NH resonances at $-0.49, -0.82,$ and -3.69 ppm (inset of Figure 2C). The protonation is accompanied by the upfield relocation of β -H pyrrole resonances.

The resonances of the appended pyrrole ring of **5** were unambiguously assigned at 5.54 (H3'), 5.82 (H4'), 6.33 (H5'), and 7.26 (NH) ppm (Figure 2A). Due to the tetrahedral geometry around the C3 atom, the two sides of the macrocyclic plane are differentiated by the position of the appended pyrrole moiety. Consequently two *ortho* and *meta* protons on each *meso*-aryl ring are nonequivalent and should present two separate resonances in the ¹H NMR spectra while the rotation about the C_{meso}–C_{ipso} bond is restricted. Even at 298 K the five well-separated, although slightly broadened, resonances were detected for the phenyl ring at the 5-position, which is adjacent to the appended pyrrole (Figure 2A). The steric hindrance increases the rotation barrier in comparison to the other *meso* positions, where single *ortho* and single *meta* multiplets were detected at 298 K. Once the temperature was lowered the dynamic processes could be detected for the other three *meso*-aryl groups. The sets of five resonances for each phenyl moiety and four for each *p*-tolyl ring were detected once the rotations were completely frozen (Figure 2B).

Formation and characterization of [(pyr)OCP]Ni^{II}] and [(pyr)OCP]Pd^{II}]: The reaction between nickel(II) chloride and **5** in acetonitrile in the presence of anhydrous K₂CO₃ resulted in formation of the green, diamagnetic, four-coordinate complex [(pyr)OCP]Ni^{II}] (**9a**). A similar procedure with palladium(II) chloride as the source of the metal ion produced the analogous green complex [(pyr)OCP]Pd^{II}] (**9b**; Scheme 6). Thus, the metal-insertion process is accompanied by a dehydrogenation step and the macrocyclic ring corresponds to the “true” oxaporphyrin **4**, although embedded into the substituted form **7**.



Scheme 6. Structures of metal complexes [(pyr)OCP]Ni^{II}] (**9a**), [(pyr)OCP]Pd^{II}] (**9b**), and [(pyr)OCP]Ag^{III}] (**9c**).

The electronic absorption spectra of **9a** and **9b** are shown in Figure 3. The spectrum of **9a** shows a set of bands of comparable intensity at 370, 473, and 490 nm accompanied by a set of less intense bands at 578, 664, 763, and 843 nm. The

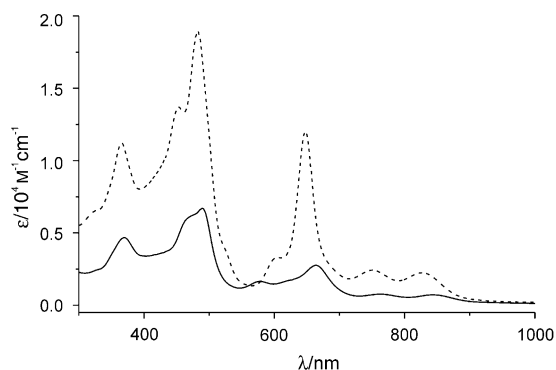


Figure 3. The electronic absorption spectra of **9a** (solid line) and **9b** (dashed line) in dichloromethane.

spectrum is completely different from that of the macrocyclic substrate **5**. Although one can detect several bands in the region typically assigned to the Soret-like band of aromatic carbaporphyrinoids, their low extinction coefficients ($\epsilon \approx 8 \times 10^3 \text{ M}^{-1} \text{ cm}^{-1}$) imply a lowering of the aromatic character of the ligand in **9a** or **9b** in comparison to that in **5**. The spectroscopic pattern for **9b** resembles that of **9a** although all bands are bathochromically shifted.

The ¹H NMR spectra of **9a** and **9b** differ essentially from the spectrum of **5** (Figure 4). The most notable feature in **9a**

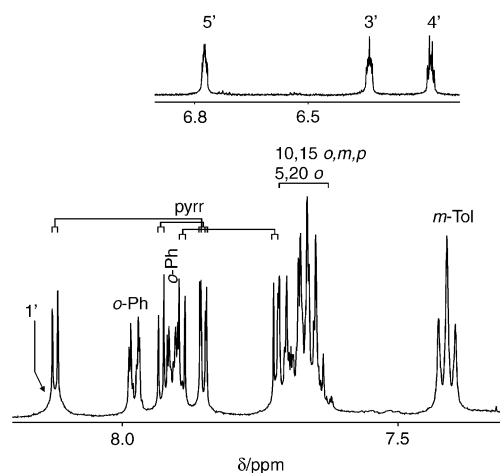


Figure 4. ¹H NMR spectra of **9a** (CD₂Cl₂, 298 K). The inset shows the resonances of the appended pyrrole.

and **9b** is the coordination through the unprotonated C21 atom of the furan ring, as inferred from the disappearance of the resonance assigned to H21. Significantly the H3 resonance, identified for **5**, is also absent in the spectra of **9a** and **9b**. Thus, the ¹H NMR spectra of **9a** and **9b** present three AB systems of β-H pyrrole protons. All pyrrole protons and all *meso*-aryl protons of **9a** and **9b** demonstrate chemical shifts that contain some downfield contribution due to the aromatic ring-current effect. The effect is significantly less pronounced than that detected for the starting macrocycle **5**. The chemical shift pattern of the pyrrole resonances closely resembles that found for nickel(II) complexes of the inverted porphyrin methylated on the outer nitrogen atom, a fact which suggests that the identical role of C21-bearing rings originated from *N*-methylated pyrrole and furan in the overall π delocalization route.^[3]

Crystal structure of [(pyr)OCP]Ni^{II}]: The structure of [(pyr)OCP]Ni^{II}] has been determined by X-ray crystallography. Perspective views of the molecule are shown in Figure 5. Table 1 contains selected bond lengths and angles. The macrocycle is only slightly distorted from planarity, as can be seen in Figure 5. The dihedral angle between the macrocyclic and the appended-pyrrole plane reflects the biphenyl-like arrangement and equals 26.4°, with the NH group pointing towards the adjacent phenyl ring on the 5-position. This value is significantly smaller than the dihedral angles between the *meso*-aryl rings and the oxacarboxyporphyrin plane (phenyl(5) 60.9°, phenyl(20) 58.6°, *p*-tolyl(10) 61.5°, *p*-tolyl(15) 54.4°). For comparison, a coplanar arrangement of pyrrole and furan rings was reported for unsubstituted simple 2-(2'-furyl)pyrrole in solution.^[35, 36]

The Ni–N distances in **9a** (Table 1) are comparable to those in the nearly planar diamagnetic nickel(II) porphyrins or porphyrinoids.^[1, 5–7, 28, 37] The Ni–C bond length of **9a** (1.892(4) Å) is in the middle range of Ni^{II}–C bond lengths (1.81–2.02 Å).^[38, 39] This bond length is similar to other nickel(II) carbaporphyrinoids where the trigonal carbon atom coordinates, for example, the nickel(II) carbaporphyrin containing the benzoindolizine-like moiety (Ni–C21

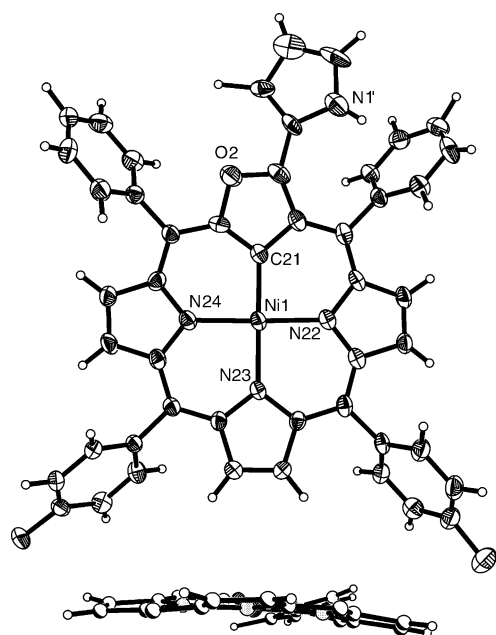


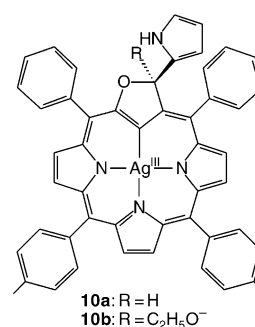
Figure 5. The X-ray crystal structure of **9a**. Top: perspective view, bottom: side view (phenyl groups omitted for clarity). The thermal ellipsoids represent 50% probability.

1.904(2) Å,^[5] nickel(II) azuliporphyrin (Ni–C21 1.897(3) Å),^[28] and [(2-BrCH₂CH₂-CTPP)Ni] (Ni–C21 1.906(4) Å).^[6] The single case where nickel(II) carbaporphyrinoids contain a coordinating tetrahedral carbon atom, [(21-CH₃CTPP)Ni^{II}], demonstrates a longer Ni–C bond length of 2.005(6) Å.^[7] Analysis of the structural data, although limited to the five available examples of nickel(II) (NNNC) carbaporphyrinoids, shows that nickel(II)–carbon(sp²) bond lengths are very similar, in spite of the different nature of the carbon-donor-bearing ring (*N*-confused pyrrole, *O*-confused furan, azulene, fused heterocycle related to benzoindolizine).

Examination of the crystallographic data demonstrated that there is some appreciable effect of the macrocyclic conjugation on the furan moiety. The C_β–C_β bond lengths are larger than those for C_α–C_β. However, the C_α–C_β distances are longer and the C_β–C_β distances are shorter than in unperturbed furan.^[40–43] These bond changes indicate that the π delocalization through the furan ring is altered. Thus, this is an intermediary situation between those where the furan ring has been built into nonaromatic and aromatic macrocycles.

Formation and characterization of [(C₂H₅O,pyr)OCP]Ag^{III}:

The reaction between silver acetate and **5** in acetonitrile resulted in the formation of [(H,pyr)OCP]Ag^{III} (**10a**; Scheme 7). In the course of metal insertion, other species, which presumably preserve the overall macrocyclic skeleton of **10a** but contain unidentified substituents on the C3 position, were detected in the ¹H NMR spectra as well. Attempts to separate **10a** by column chromatography continually led to a variety of derivatives due to the intrinsic reactivity at the C3 position. Once ethanol was introduced on purpose, [(C₂H₅O,pyr)OCP]Ag^{III} (**10b**), which is structurally



Scheme 7. Structures of metal complexes [(H,pyr)OCP]Ag^{III} (**10a**) and [(C₂H₅O,pyr)OCP]Ag^{III} (**10b**).

related to **10a**, was exclusively obtained. The compound sustained the chromatographic purification to give an overall 78% yield of insertion.

The electronic absorption spectrum of **10b** (Figure 6) with its intense Soret-like band (443 nm in CH₂Cl₂) and a set of bands in the Q region is similar to the spectrum of the free ligand, which implies that **10b** conserves the basic chromophore of **5** (Figure 1).

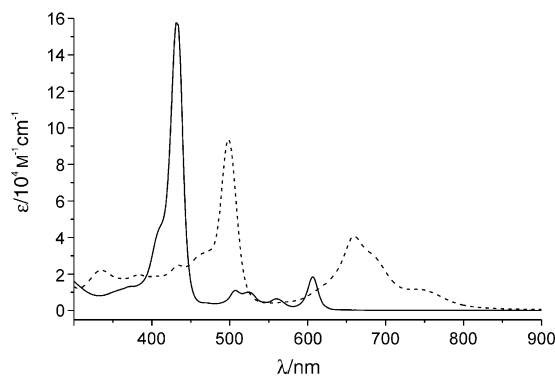


Figure 6. The electronic absorption spectra of **10b** (solid line) and **9c** (dashed line) in dichloromethane. The figure presents the starting and final points of titration of **10b** with TFA.

The ¹H NMR spectra of **10a** and **10b** bear a strong resemblance to the spectrum of the free ligand **5**; thereby proving that the macrocyclic frame of **5** is conserved in **10a** and **10b**. Due to the coordination, the H21 and two inner NH resonances seen for **5** are absent. The H3 atom has been replaced by an ethoxy substituent. Consequently, the diagnostic set of two complex multiplets at 3.84 and 3.19 ppm was assigned to the ethoxy methylene group (inset A2 in Figure 7A). The strong difference of the chemical shifts detected for the two methylene multiplets is due to the diastereotopic effect as the chirality center is created on the tetrahedral hybridized C3 atom. The structurally informative H3 resonance for **10a** was identified at 8.08 ppm.

Coordination through the nitrogen donors in **10b** is reflected by the presence of ^{107/109}Ag scalar splitting, seen for the H7, H8, H17, and H18 β-H pyrrolic signals. In each case the coupling constant ⁴J_{AgH} equals 1.5 Hz (inset A1 in Figure 7A). Such a coupling was not detected for the H12 and H13 resonances of the central pyrrole ring.

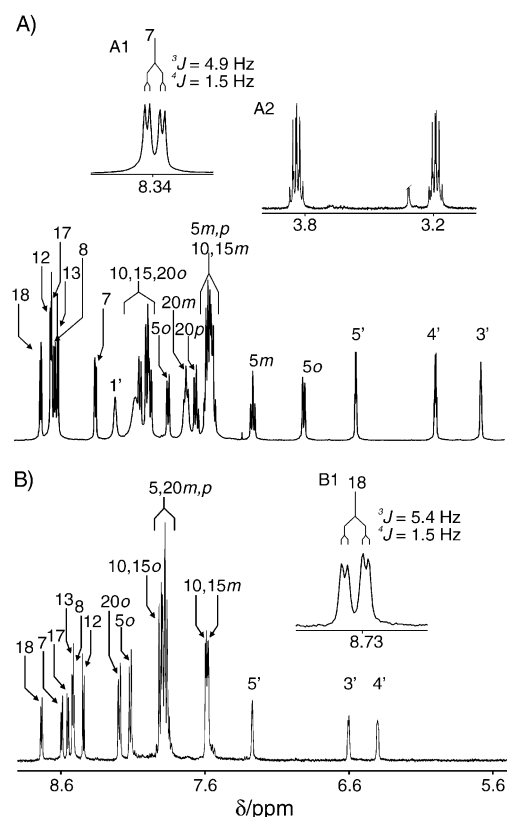


Figure 7. ^1H NMR spectra of: A) **10b** (CD_2Cl_2 , 298 K) and B) **9c** (CD_2Cl_2 , 298 K). Insets A1 and B1 (not to scale) present the β -H resonances showing couplings to $^{107/109}\text{Ag}$. The diastereotopic splitting of the CH_2 resonances of the ethoxy group on the 3-position is shown in inset A2.

The ethoxy substituent on the 3-position of **10b** could be replaced by a methoxy group by addition of TFA followed by treatment with sodium methoxide to yield $[(\text{CH}_3\text{O},\text{pyr})\text{OCP}]\text{Ag}^{\text{III}}$; this was reflected by an OCH_3 resonance at 3.30 ppm. The unique, diastereotopically split ethoxy multiplets were replaced by the typical quartet of the methylene group of free ethanol. A related exchange was previously detected in the case of cobalt(II) methoxybiliverdin complexes.^[44]

Crystal structure of $[(\text{C}_2\text{H}_5\text{O},\text{pyr})\text{OCP}]\text{Ag}^{\text{III}}$ (10b**):** The structure of **10b** has been determined by X-ray crystallography. The perspective views of the molecule are shown in Figure 8. The macrocycle is only slightly distorted from planarity, as can be seen in Figure 8. The tetrahedral geometry around the C3 atom is demonstrated by the respective bond angle values. Table 1 contains selected bond lengths and angles.

The Ag–N and Ag–C distances (Table 1) are comparable to those in other silver(III) carbaporphyrinoids, for example, silver(III) inverted porphyrin (Ag–N22 2.06(2), Ag–N23 2.08(2), Ag–N24 2.03(2), and Ag–C21 2.04(2) Å),^[13] silver(III) benzocarbaporphyrin (Ag–N22 2.038(4), Ag–N23 2.084(4), Ag–N24 2.046(4), and Ag1–C21 2.015(4) Å),^[29] and silver(III) double *N*-confused porphyrin (Ag–C21 2.011(7), Ag–C22 1.987(2), Ag–N23 2.064(5), and Ag–N24 2.047(7) Å).^[45]

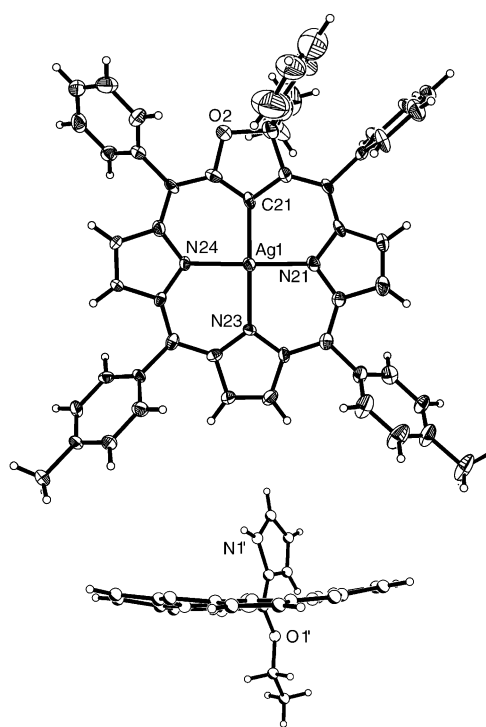


Figure 8. The crystal structure of **10b**. Top: perspective view, bottom: side view (phenyl groups omitted for clarity). The thermal ellipsoids represent 50% probability.

Table 1. Selected bond lengths and angles.

Compound	Bond lengths [Å]	Angles [°]
$[(\text{pyr})\text{OCP}]\text{Ni}^{\text{II}}$ (9a)	Ni1–N22 1.945(4) Ni1–N23 1.952(4) Ni1–N24 1.975(4) Ni1–C21 1.892(4)	C21–Ni1–N22 88.5(2) C21–Ni1–N23 178.1(2) N22–Ni1–N23 91.2(2) C21–Ni1–N24 90.1(2) N22–Ni1–N24 177.9(2) N23–Ni1–N24 90.2(2)
$[(\text{C}_2\text{H}_5\text{O},\text{pyr})\text{OCP}]\text{Ag}^{\text{III}}$ (10b)	Ag1–N22 2.031(5) Ag1–N23 2.069(5) Ag1–N24 2.042(5) Ag1–C21 2.020(7)	C21–Ag1–N22 89.4(2) C21–Ag1–N24 89.3(2) N22–Ag1–N24 178.5(2) C21–Ag1–N23 179.5(3) N22–Ag1–N23 90.2(2) N24–Ag1–N23 91.1(2) O1'–C3–O2 106.3(6) O1'–C3–C1' 104.9(7) O2–C3–C1' 107.1(6) O1'–C3–C4 116.7(6) O2–C3–C4 105.0(5) C1'–C3–C4 116.1(6)

The comparison of the structural data, although limited to the three available examples of silver(III) (NNNC) carbaporphyrinoids, shows that silver(III)–carbon(sp^2) bond lengths are very similar in spite of the different nature of the carbon-donor-bearing ring (related to *N*-confused pyrrole, substituted *O*-confused furan, or indene).

Formation and characterization of $[(\text{pyr})\text{OCP}]\text{Ag}^{\text{III}}$ (9c**):** The ^1H NMR titration of $[(\text{C}_2\text{H}_5\text{O},\text{pyr})\text{OCP}]\text{Ag}^{\text{III}}$ **10b** with TFA in CD_2Cl_2 was carried out. Under these conditions **10b** is readily transformed into the new aromatic complex $[(\text{pyr})\text{OCP}]\text{Ag}^{\text{III}}$ (**9c**; Scheme 6), through an exocyclic C3–O

bond cleavage followed by an elimination of the ethoxy group. Formally, the complex **9c** can be produced by the insertion of a silver(III) cation into hypothetical compound **8** (Scheme 5), with the replacement of H21 and an inner NH proton. Addition of sodium ethoxide in ethanol to the solution of **9c** reverses the course of the titration to recover starting material **10b**.

The observed changes in the electronic absorption spectra are consistent with an equilibrium between two species, as the well-defined sets of isosbestic points have been detected. The electronic absorption spectrum of **9c** is completely different from that of starting material **10b**; it does, however, resemble that of **9a** or **9b** (Figure 6). The spectrum shows the intense, Soret-like band at 498 nm accompanied by the comparable ones at 660, 684, and 747 nm; this indicates coupling between two conjugated moieties. The chromophore undergoes fundamental structural changes, in relation to **10b**, that approach the structure seen for **9a**.

In contrast to the marked changes seen in the electronic absorption spectra, relatively small changes of the ^1H NMR chemical shifts were observed in comparison to **10b**, a fact which is clearly consistent with the macrocyclic aromaticity of the ligand in **9c**. The fine structure of β -H resonances seen for parental **10b** due to the coupling with $^{107/109}\text{Ag}$ was conserved. The NH1' resonance was identified at 9.81 ppm. The marked unequivalence of the *ortho* and *meta* resonances, characteristic for **10b**, disappeared over the whole investigated temperature range of 203–293 K. In the course of titration with TFA, the diastereotopically split, ethoxy methylene multiplet was gradually replaced by the quartet signal of free ethanol. Importantly, one equivalent of ethyl alcohol was released, as confirmed by careful integration of the alcohol resonances with respect to those of **9c**.

The spectroscopic data can be accounted for by the structure presented in the Scheme 6. The elimination of the ethoxy group allows a similar arrangement of whole macrocycle and the appended pyrrole ring as is seen in **9a**, with the relatively small dihedral angle between the macrocyclic plane and the appended pyrrole plane but with the NH group oriented toward the O2 atom. The unequivalency of the two 2-oxa-21-carbaporphyrin sides, seen for **10b**, has been removed in **9c**, thereby rendering the *ortho* and *meta* protons of the *meso*-phenyl groups equivalents. The critical insight into the molecular structure of **9c** was given by COSY and NOESY studies. Considering in detail the spatial proximity of H3' and H4' to the *ortho* proton of the phenyl on C5 and the larger distance between H5' and the *ortho* proton of the same phenyl group, one would expect strong NOE cross-peaks to occur exclusively between the first two couples, as was detected.

Remarkable changes of the appended-pyrrole ^1H NMR pattern have been observed in **9a–c** (Table 2). The marked downfield relocation of the resonances of **9a–c** with respect to those of **10b** is the most analytically important. The reasons for the changes are complex. The simultaneous modification of the macrocyclic ring current and/or electronic structure of the appended fragment are of importance. Definitely a different ring-current effect is sensed by the appended pyrrole

Table 2. Appended-pyrrole ^1H (^{13}C) NMR chemical shift values [ppm].

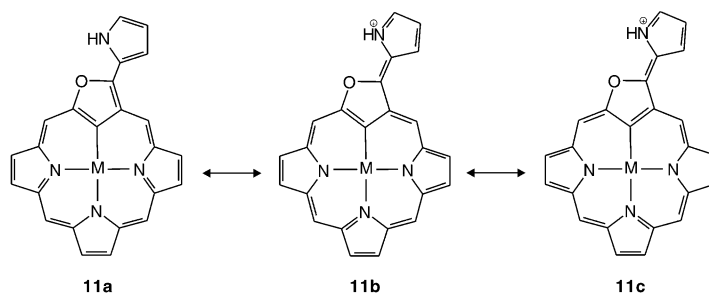
Compound	Position			
	3'	4'	5'	NH
pyrrole ^[46]	6.22 (108.2)	6.22 (108.2)	6.68 (118.5)	
[(H ₂ pyr)OCPH]H ₂ (5)	5.54 (109.8)	5.82 (108.5)	6.33 (118.5)	7.26
[(H ₂ pyr)OCPH]H ₂ ⁺ (5-H⁺)	5.91 (111.5)	5.69 (107.6)	5.99 (120.1)	7.69
[(C ₂ H ₅ O ₂ pyr)OCP]Ag ^{III} (10b)	5.66 (107.4)	5.98 (108.9)	6.53 (116.6)	8.20
[(pyr)OCP]Ni ^{III} (9a)	6.34 (119.2)	6.17 (111.9)	6.76 (126.4)	8.10
[(pyr)OCP]Pd ^{III} (9b)	6.36 (120.4)	6.20 (112.1)	6.79 (127.2)	8.16
[(pyr)OCP]Ag ^{III} (9c)	6.60 (125.9)	6.40 (115.4)	7.27 (133.9)	9.81
dipyrrromethene ^[47]	6.64 (128.8)	6.39 (117.2)	7.63 (143.1)	

of the two silver(III) complexes, due its different orientation with respect to the macrocyclic plane.

The analysis of the ^{13}C chemical shifts (Table 2) provides an essential insight into the different role of the pyrrole fragment and underscores the direct electronic effects. The ring-current contributions to overall changes in ^{13}C NMR chemical shifts are negligible. For the sake of comparison, the respective chemical shift values of free pyrrole^[46] and the conjugated pyrrole ring of 5-anisol-dipyrrromethene^[47] have been included in Table 2. These values set the spectroscopic standards for two extreme structures of the appended pyrrole. Actually, representative ^{13}C chemical shifts for a conjugated pyrrole have also been reported for other molecules, that is, ruthenium complexes containing butatrienylidene (C3' 125.2, C4' 112.8, and C5' 140.5 ppm)^[48] and bis-dipyrrromethenes (C5' 141.1 ppm).^[49]

The ^{13}C NMR chemical shifts found for the appended-pyrrole resonances of **5**, **10a**, and **10b** are fairly typical of unperturbed pyrrole. These values are similar to relevant shifts seen for 2-aza-3-(2'-pyrrolyl)-5,10,15,20-tetraphenyl-21-carbaporphyrin.^[34] The ^{13}C chemical shifts seen for **9** increase systematically in the series **9a**, **9b**, **9c** to approach the limits of 5-phenyl-dipyrrromethene. The trend can be rationalized by an effective conjugation between the macrocycle and the appended pyrrole moiety. In terms of ^{13}C chemical shifts, it is clear that the extent of the conjugation is dependent on the charge of the coordinated metal ions, with the largest effect being seen for **9c**.

To account for the structural and spectroscopic characteristics of **9a–c**, one can formally include a set of canonical structures **11a–c** (Scheme 8). The Kekulé structure of **11a** defines the metallocarbaporphyrinoid molecule where, for topological reasons, the macrocyclic aromaticity typical of porphyrin can not be retained. On the other hand, for **11b** and **11c** the 18 electron π -delocalization pathway allows macrocyclic aromaticity. Direct π conjugation between the append-

Scheme 8. The set of formal canonical structures **11a–c**.

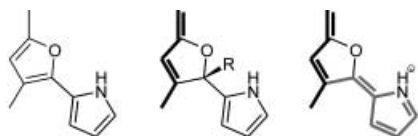
ed pyrrole fragment and the carbaporphyrinoid π system is expected in **11b** and **11c**. The exocyclic double bond connects the C3 and C2' atoms, with the presumption that the appended pyrrole ring is in the plane of the 2-oxa-21-carbaporphyrin. Consequently, the appended moiety can participate in the overall π delocalization. In reality, the evolution of the conjugative effect when going from planar to perpendicular conformations is expected, with the largest effect for the coplanar arrangement. It is worth noting that the relatively small dihedral angle between the pyrrole and furan plane in **9b** suggests the contribution of conjugation in the determination of the macrocyclic structure. In this consideration, we have taken into account the extensive interannular conjugation in the description of the electronic and molecular structure of 2-(2'-furyl)pyrrole alone, which adopts a *cis*-planar conformation in solution.^[35, 36] The conjugation between the pyrrole group and the aromatic macrocycle can be related to that described for 2-(2'-furyl)pyrrole by presuming that the furan ring, built into the 2-oxa-21-carbaporphyrin structure, acts as an efficient bridge between the macrocycle and the appended pyrrole.

Consequently, the electronic structures of **9a–c** can be described by a combination of aromatic and nonaromatic canonical structures, which participate in the overall picture in proportions imposed by the charge of the central metal ion. Clearly, the definitely aromatic character of the 2-oxa-21-carbaporphyrin macrocycle in **9c** is consistent with a dominating contribution of **11b** and **11c**. On the other hand, the participation of **11a** is strongly marked for **9a** and **9b**.

Conclusion

In the present work we have described the synthesis and reactivity of a new carbaporphyrinoid. The molecule has been constructed by applying the heteroatom confusion concept. An interchange of an oxygen atom with a β -methine group of furan transforms 5,10,15,20-tetraaryl-21-oxaporphyrin into 5,10,15,20-tetraaryl-2-oxa-21-carbaporphyrin. Inherent reactivity of the furan ring in the presence of pyrrole required during the course of the synthesis prevented formation of the "pure" *O*-confused oxaporphyrin. Instead, the procedure resulted in a modified macrocycle, which was, however, directly related to the *O*-confused oxaporphyrin.

The new molecule, applied as a ligand toward selected metal ions, reveals the peculiar plasticity of its molecular and electronic structure. The structural changes are easily triggered by addition/elimination of a nucleophile at the C3 position (Scheme 9). The tetrahedral–trigonal rearrangements originate at the C3 atom but the consequences extend



Scheme 9. Addition/elimination of a nucleophile at C3 triggers the structural changes.

over the whole structure. This important feature of *O*-confused porphyrin derivatives has enabled us to investigate and eventually to control the subtle interplay between their structural flexibility, perimeter substitution, coordination, and aromaticity. Essentially the oxidation of the central metal ion can be considered as a factor that determines the molecular structure of the ligand. The dianionic or trianionic macrocyclic core of the pyrrole-appended derivatives is favored to match the oxidation state of nickel(II), palladium(II), or silver(III), respectively.

In general the coordinating environment provided by carbaporphyrinoids offers a unique opportunity to create novel organometallic compounds and to control their reactivity. Thus, an original route to tune carbaporphyrinoids to the coordination requirements of metal ions through a 2-(2'-furyl)pyrrole moiety has been introduced.

Experimental Section

Materials: 3-Furaldehyde, phenyl Grignard reagent, *s*BuLi, and *n*BuLi (all from Aldrich) were used as received.

2-(Phenylhydroxymethyl)-4-furaldehyde: *n*BuLi (23.91 mL, 38.25 mmol, 1.6 M solution in hexanes) was added to morpholine (3.33 mL, 38.25 mmol) in THF (150 mL) at -78°C .^[32] 3-Furaldehyde (3 mL, 36.4 mmol) was added after 20 min, to be followed after a further 20 min by *s*BuLi (29.4 mL, 38.25 mmol, 1 M solution in hexanes). The resulting mixture was stirred for 4 h at -78°C . After that time benzaldehyde (4.08 mL, 40.05 mmol) was added and the reaction was left for 16 h while the cooling bath reached room temperature. The mixture was poured into hydrochloric acid/ice (1:10 *v/v*). The organic products were extracted with diethyl ether (three times). All organic layers were collected, dried with MgSO_4 , and filtered. The solvents were evaporated under reduced pressure. The residue was dissolved in benzene and purified by chromatography through a basic alumina column. The first orange fraction to be eluted with benzene was collected, and the solvent was removed with a vacuum rotary evaporator to give 2-(phenylhydroxymethyl)-4-furaldehyde as an orange oil (3.6 g, 50%). $^1\text{H NMR}$ (500.13 MHz, CDCl_3): $\delta = 9.81$ (s, 1H), 7.97 (s, 1H), 7.41–7.31 (m, 5H), 6.49 (s, 1H), 5.78 (s, 1H), 2.82 (s, 1H) ppm; $^{13}\text{C NMR}$ (125.77 MHz, CDCl_3): $\delta = 184.5$, 158.8, 151.2, 139.8, 128.6, 128.5, 126.5, 104.4, 69.8 ppm; MS: *m/z*: calcd for $\text{C}_{12}\text{H}_9\text{O}_2^+$ [$M - \text{OH}$] $^+$: 185.06; found: 185.1.

2,4-Bis(phenylhydroxymethyl)furan (3): 2-(Phenylhydroxymethyl)-4-furaldehyde (500 mg, 2.5 mmol) was dissolved in freshly distilled THF (100 mL). PhMgBr (1.5 mL, 3 M solution in diethyl ether) was added through a syringe. The resulting mixture was stirred for 30 min, and 1% H_2SO_4 (40 mL) was added. The solution was neutralized by addition of Na_2CO_3 until the liberation of CO_2 ceased. The product was extracted with diethyl ether (three times). All organic layers were collected, dried with MgSO_4 , filtered, and evaporated with a vacuum rotary evaporator. Product **3** was obtained almost quantitatively as an orange oil. $^1\text{H NMR}$ (500.13 MHz, CDCl_3): $\delta = 7.71$ –7.31 (m, 10H), 7.22 (d, 1H), 6.07 (d, 1H), 5.74 (s, 1H), 5.68 (s, 1H), 2.37 (s, 1H), 2.11 (s, 1H) ppm; $^{13}\text{C NMR}$ (125.77 MHz, CDCl_3): $\delta = 156.8$, 142.8, 140.5, 139.7, 128.7, 128.5, 128.4, 128.1, 127.9, 127.2, 127.1, 126.6, 126.3, 106.98, 70.1, 69.8 ppm; MS: *m/z*: calcd for $\text{C}_{18}\text{H}_{15}\text{O}_2^+$ [$M - \text{OH}$] $^+$: 263.1; found: 263.3.

[(H₂pyr)OCPH]₂ (5): Compound **3** (280 mg, 1 mmol), pyrrole (208 μL , 3 mmol), and *p*-toluylaldehyde (236 mL, 2 mmol) were dissolved in freshly distilled dichloromethane (100 mL). N_2 gas was bubbled through the solution for 20 min to remove oxygen before $\text{BF}_3 \cdot \text{Et}_2\text{O}$ (37 μL) was added. The solution was stirred for 1 h in the absence of light, DDQ (681 mg, 3 mmol) was added, and the solution was stirred for an additional 20 min. The solvent was removed with a vacuum rotary evaporator. The dark residue was separated by chromatography on a basic alumina (grade II) column. The fast-moving fraction was collected and immediately separated again by chromatography on a silica gel (mesh 35–70) column. The product was eluted with dichloromethane as a slow-moving, brown band.

Recrystallization from dichloromethane/methanol (50:50 v/v) gave **5** (70 mg, 10%). $^1\text{H NMR}$ (500.13 MHz, CD_2Cl_2): δ = 8.49 (d, 1H, 3J = 4.9 Hz), 8.47 (d, 1H, 3J = 4.9 Hz), 8.47 (d, 1H, 3J = 4.6 Hz), 8.45 (d, 1H, 3J = 4.6 Hz), 8.44 (d, 1H, 3J = 4.9 Hz), 8.29 (d, 1H, 3J = 4.9 Hz), 8.10 (d, 2H, 3J = 7.6 Hz), 8.08 (s, 1H), 8.04 (m, 3H), 7.96 (m, 3H), 7.69 (t, 2H), 7.53 (m, 6H), 7.38 (brs), 7.26 (s, 1H), 7.21 (brs), 6.33 (m, 1H), 5.82 (m, 1H), 5.54 (m, 1H), 2.67 (s, 3H), 2.66 (s, 3H), –5.11 (s, 1H) ppm; $^{13}\text{C NMR}$ (125.77 MHz, CDCl_3): δ = 160.3, 152.9, 152.4, 143.3, 140.4, 139.9, 139.4, 139.3, 139.3, 139.2, 138.4, 137.3, 137.3, 137.2, 135.1, 134.5, 134.3, 134.3, 134.2, 134.1, 134.0, 133.8, 133.6, 132.1, 131.8, 130.8, 130.1, 127.9, 127.6, 127.5, 127.4, 127.3, 127.2, 126.4, 126.3, 123.1, 123.0, 121.2, 120.4, 120.1, 117.9, 112.5, 109.3, 108.2, 106.4, 105.2, 85.3, 21.5, 21.5 ppm; UV/Vis: λ_{max} (log ϵ) = 437 (5.01), 533 (3.96), 567 (3.81), 622 (3.58), 679 (3.84) nm; HRMS: m/z : calcd for $\text{C}_{50}\text{H}_{39}\text{N}_4\text{O}_1 [M+\text{H}]^+$: 711.3124; found: 711.3118; elemental analysis calcd (%) for $\text{C}_{50}\text{H}_{38}\text{N}_4\text{O}_1 \cdot (\text{with } 0.33 \text{ CH}_2\text{Cl}_2)$: C 81.95, H 5.24, N 7.59; found: C 81.65, H 5.36, N 7.65.

[(C₂H₅O₂pyr)OCP]Ag^{III} (10b**):** Compound **5** (15 mg, 0.021 mmol) was dissolved in chloroform (20 mL), and silver acetate (146 mg) in acetonitrile (20 mL) was added. The mixture was heated to reflux for 30 min, then the solvent was removed with a vacuum rotary evaporator. The solid residue was immediately separated on a silica gel (mesh 35–70) column. The red fraction was eluted with toluene. The solvent was removed in a stream of nitrogen. Recrystallization from chloroform/methanol (50:50 v/v) gave **10b** (13.4 mg, 78%). $^1\text{H NMR}$ (500.13 MHz, CD_2Cl_2): δ = 8.72 (dd, 1H, 3J = 4.9, $^4J_{\text{Ag}}$ = 1.1 Hz), 8.65 (d, 1H, 3J = 4.6), 8.64 (dd, 1H, 3J = 4.9, $^4J_{\text{Ag}}$ = 1.5 Hz), 8.62 (dd, 1H, 3J = 4.9, $^4J_{\text{Ag}}$ = 1.1 Hz), 8.60 (d, 1H, 3J = 4.6 Hz), 8.34 (dd, 1H, 3J = 4.9, $^4J_{\text{Ag}}$ = 1.5 Hz), 8.20 (s, 1H), 8.05 (m, 3H), 7.97 (m, 3H), 7.84 (m, 1H), 7.71 (t, 2H), 7.64 (m, 1H), 7.59–7.49 (m, 6H), 7.25 (td, 1H, J = 7.6, 1.5 Hz), 6.89 (m, 1H), 6.53 (m, 1H), 5.98 (m, 1H), 5.66 (m, 1H), 3.84 (m, 1H), 3.19 (m, 1H), 2.68 (s, 3H), 2.67 (s, 3H), 1.20 (t, 3H) ppm; $^{13}\text{C NMR}$ (125.77 MHz, CD_2Cl_2): δ = 148.1, 142.1, 142.1, 140.3, 140.3, 139.4, 139.3, 139.0, 138.5, 138.1, 138.1, 137.0, 136.8, 135.6, 134.7, 133.9, 133.9, 133.9, 133.8, 133.6, 133.3, 132.4, 129.8, 129.3, 129.3, 128.9, 128.9, 128.5, 128.1, 128.1, 128.1, 128.0, 127.8, 127.3, 127.2, 126.4, 126.1, 125.5, 125.5, 121.9, 121.8, 118.4, 118.3, 116.6, 111.9, 109.7, 109.7, 108.0, 107.4, 59.2, 21.6, 21.6, 15.1 ppm; UV/Vis: λ_{max} (log ϵ) = 432 (5.19), 508 (4.02), 524 (3.97), 560 (3.77), 607 (4.21) nm; HRMS: m/z : calcd for $\text{C}_{52}\text{H}_{39}\text{N}_4\text{O}_2\text{Ag} [M]^+$: 858.2123; found: 858.2118.

[(pyr)OCP]Ni^{II} (9a**):** Compound **5** (20 mg, 0.028 mmol), NiCl_2 (36.6 mg, 0.28 mmol), and K_2CO_3 (excess) were added to acetonitrile (25 mL). The mixture was heated to reflux for 1.5 h. The solvent was removed under reduced pressure. The remaining solid was dissolved in freshly distilled dichloromethane and separated by chromatography on a silica gel (Mesh 35–70) column. The fast-moving, green band was collected. Recrystallization from $\text{CHCl}_3/\text{MeOH}$ gave **9** (8.6 mg, 40%). $^1\text{H NMR}$ (500.13 MHz, CD_2Cl_2): δ = 8.12 (d, 1H, 3J = 4.9 Hz), 8.10 (s, 1H), 7.98 (m, 2H), 7.93 (d, 1H, 3J = 4.9 Hz), 7.90 (m, 2H), 7.89 (d, 1H, 3J = 3.8 Hz), 7.86 (d, 1H, 3J = 4.9 Hz), 7.85 (d, 1H, 3J = 4.9 Hz), 7.72 (d, 1H, 3J = 3.8 Hz), 7.71 (m, 2H), 7.68–7.63 (m), 7.41 (m, 4H), 6.76 (m, 1H), 6.34 (m, 1H), 6.17 (m, 1H), 2.58 (s, 3H), 2.56 (s, 3H) ppm; $^{13}\text{C NMR}$ (125.77 MHz, CD_2Cl_2): δ = 164.5, 154.3, 151.3, 150.9, 149.4, 149.1, 147.9, 146.1, 141.8, 138.5, 138.3, 137.6, 137.6, 137.6, 134.8, 134.3, 133.8, 133.7, 133.3, 131.6, 131.5, 130.9, 129.3, 129.2, 128.3, 128.1, 128.1, 127.8, 127.7, 127.5, 126.5, 124.4, 123.0, 122.9, 121.9, 119.7, 119.2, 117.3, 111.9, 21.6, 21.5 ppm; UV/Vis: λ_{max} (log ϵ) = 370 (3.75), 473 (3.87), 490 (3.90), 578 (3.29), 664 (3.52), 763 (2.96), 843 (2.93) nm; HRMS: m/z : calcd for $\text{C}_{50}\text{H}_{34}\text{N}_4\text{O}_1\text{Ni} [M]^+$: 764.2086; found: 764.2081.

[(pyr)OCP]Pd^{II} (9b**):** Compound **5** (15.5 mg, 0.022 mmol), PdCl_2 (5.5 mg, 0.032 mmol), and K_2CO_3 (excess) were added to acetonitrile (25 mL). The mixture was heated to reflux for 1.5 h. The solvent was removed under reduced pressure. The remaining solid was dissolved in freshly distilled dichloromethane and separated by chromatography on a silica gel (mesh 35–70) column. The fast-moving, green band was collected. Recrystallization from $\text{CHCl}_3/\text{MeOH}$ (50:50 v/v) gave **9b** (12 mg, 68%). $^1\text{H NMR}$ (500.13 MHz, CD_2Cl_2): δ = 8.16 (s, 1H), 8.12 (d, 1H, 3J = 4.9 Hz), 8.05 (m, 2H), 7.96 (m, 2H), 7.92 (d, 1H, 3J = 4.9 Hz), 7.90 (d, 1H, 3J = 4.9 Hz), 7.87 (d, 1H, 3J = 4.9 Hz), 7.82 (d, 1H, 3J = 4.9 Hz), 7.80 (d, 1H, 3J = 4.9 Hz), 7.77 (m, 2H), 7.75–7.67 (m), 7.43 (m, 4H), 6.79 (m, 1H), 6.36 (m, 1H), 6.20 (m, 1H), 2.60 (s, 3H), 2.58 (s, 3H) ppm; $^{13}\text{C NMR}$ (125.77 MHz, CD_2Cl_2): δ = 167.6, 153.5, 151.6, 150.1, 149.2, 148.5, 147.7, 145.3, 141.5, 139.7, 139.5, 136.8, 135.9, 135.8, 135.4, 135.4, 135.2, 134.6, 132.8, 132.7, 132.5, 132.4, 131.3, 131.2, 130.4, 130.1, 130.1, 129.9, 129.7, 129.6, 129.2, 126.6, 126.5, 123.1, 122.5, 122.4, 122.3, 120.6, 114.1, 23.4, 23.4 ppm; UV/Vis: λ_{max} (log ϵ) = 365 (4.28), 454 (4.36), 483 (4.51), 605 (3.75), 648 (4.31), 751 (3.61), 827

(3.58) nm; HRMS: m/z : calcd for $\text{C}_{50}\text{H}_{34}\text{N}_4\text{O}_1\text{Pd} [M]^+$: 812.1785; found: 812.1765.

[(pyr)OCP]Ag^{III} (9c**):** Compound **10b** (20 mg) was dissolved in freshly distilled dichloromethane (15 mL). A solution of TFA in dichloromethane (60%) was added through a syringe until the color changed from red to green. The product was precipitated from the reaction mixture with hexane (17.5 mg, 82%). $^1\text{H NMR}$ (500.13 MHz, CD_2Cl_2): δ = 9.54 (brs), 8.73 (dd, 1H, 3J = 5.4, $^4J_{\text{Ag}}$ = 1.5 Hz), 8.59 (dd, 1H, 3J = 4.9, $^4J_{\text{Ag}}$ = 1.5 Hz), 8.55 (d, 1H, 3J = 4.9 Hz), 8.52 (d, 1H, 3J = 4.9 Hz), 8.51 (dd, 1H, 3J = 5.3, $^4J_{\text{Ag}}$ = 1.5 Hz), 8.44 (d, 1H, 3J = 4.9 Hz), 8.19 (m, 2H), 8.12 (m, 2H), 7.89 (m, 10H), 7.58 (m, 4H), 7.27 (s, 1H), 6.60 (d, 1H), 7.68–7.63 (m), 6.40 (m, 1H), 2.68 (s, 3H), 2.67 (s, 3H) ppm; $^{13}\text{C NMR}$ (125.77 MHz, CD_2Cl_2 , partial data): δ = 131.9 (18-C), 133.5 (7-C), 130.8 (17-C), 134.4 (13-C), 132.4 (8-C), 132.2 (12-C), 134.6 (20-*o*-C), 133.5 (5-*o*-C), 133.9 (10,15-*o*-C), 130.6 (5,20-*m*-C), 129.8 and 128.6 (5,20-*p*-C), 128.8 (10,15-*m*-C), 133.9 (5'-C), 125.9 (3'-C), 115.3 (4'-C), 21.5 (10,15-*p*-CH₃) ppm; UV/Vis: λ_{max} (log ϵ) = 335 (4.29), 384 (4.23), 499 (4.92), 660 (4.55), 683 (4.43), 749 (4.00) nm; HRMS: m/z : calcd for $\text{C}_{50}\text{H}_{34}\text{N}_4\text{O}_1\text{Ag} [M]^+$: 813.1783; found: 813.1778; elemental analysis calcd (%) for $\text{C}_{52}\text{H}_{34}\text{N}_4\text{O}_3\text{F}_3\text{Ag}_1 \cdot (\text{with } 1.33 \text{ CH}_2\text{Cl}_2)$: C 61.61, H 5.33, N 5.39; found: C 61.72, H 3.32, N 5.49.

Instrumentation: NMR spectra were recorded on a Bruker Avance 500 spectrometer. Absorption spectra were recorded on a diode array Hewlett Packard 8453 spectrometer. Mass spectra were recorded on an AD-604 spectrometer by using the electrospray and liquid-matrix secondary-ion mass spectrometry techniques.

X-ray data collection and refinement: Crystals of **9a** and **10b** were prepared by diffusion of methanol into dichloromethane (**9a**) and toluene (**10b**) solutions, respectively, contained in a thin tube. Data were collected at 100 K on a Kuma KM-4 CCD diffractometer. The data were corrected for Lorentz and polarization effects. No absorption correction was applied.

Table 3. Crystal data for [(pyr)OCP]Ni^{II} (**9a**) and [(C₂H₅O₂pyr)OCP]Ag^{III} (**10b**).

	Compound	
	[(pyr)OCP]Ni ^{II}	[(C ₂ H ₅ O ₂ pyr)OCP]Ag ^{III} · 0.5 C ₂ H ₈
crystals grown by slow diffusion of	MeOH into CH ₂ Cl ₂	MeOH into toluene
crystal habit	deep green block	dark red plate
formula	C ₅₀ H ₃₄ N ₄ O ₁ Ni	C ₅₂ H ₃₉ N ₄ O ₂ Ag
<i>M_w</i>	765.52	859.74
<i>a</i> [Å]	10.2928(7)	11.1748(13)
<i>b</i> [Å]	23.7004(17)	14.5887(18)
<i>c</i> [Å]	14.7332(10)	14.8542(17)
α [°]		63.094(12)
β [°]	97.953(6)	79.353(10)
γ [°]		88.349(10)
<i>V</i> [Å ³]	3559.5(4)	2118.1(4)
<i>Z</i>	4	2
ρ_{calcd} [g cm ⁻³]	1.348	1.428
crystal system	monoclinic	triclinic
space group	<i>P</i> 2 ₁ / <i>c</i>	<i>P</i> 1̄
μ [mm ⁻¹]	0.593	0.522
absorption correction	not applied	not applied
<i>T</i> [K]	100(2)	100(2)
θ range	3.31 ≤ θ ≤ 28.55	3.27 ≤ θ ≤ 28.52
<i>hkl</i> range	– 8 ≤ <i>h</i> ≤ 13 – 31 ≤ <i>k</i> ≤ 31 – 19 ≤ <i>l</i> ≤ 19	– 14 ≤ <i>h</i> ≤ 14 – 18 ≤ <i>k</i> ≤ 18 – 17 ≤ <i>l</i> ≤ 19
reflections:		
measured	8320	9296
unique, <i>I</i> > 2 σ (<i>I</i>)	4638	4637
parameters/restraints	606/0	597/0
<i>S</i>	1.115	0.950
<i>R</i> 1 ^[a]	0.0909	0.0814
<i>wR</i> 2 ^[b]	0.1844	0.1767

[a] $R1 = \sum ||F_o - F_c| | / \sum |F_o|$. [b] $wR2 = [\sum w(F_o^2 - F_c^2)^2] / \sum w(F_o^2)^2]^{1/2}$.

Crystal data are compiled in Table 3. The structures were solved by the heavy atom method (**9a**) and direct methods (**10b**) with SHELXS-97 and refined by the full-matrix least-squares method by using SHELXL-97 with anisotropic thermal parameters for the non-hydrogen atoms. Scattering factors were those incorporated in SHELXS-97.^[50, 51] In the structure of **10b** the high-temperature factors of some appended pyrrole and ethoxy group atoms suggest disorder, which could not be resolved.^[50] Crystallographic data (excluding structure factors) have been deposited with the Cambridge Crystallographic Data Centre as supplementary publication nos. CCDC-205271 and -205272. Copies of the data can be obtained free of charge on application to CCDC, 12 Union Road, Cambridge CB21EZ, UK (fax: (+44) 1223-336-033; email: deposit@ccdc.cam.ac.uk).

Acknowledgement

Financial support from the State Committee for Scientific Research KBN of Poland (Grant: 4T09A 14722) is gratefully acknowledged.

- [1] P. J. Chmielewski, L. Latos-Grażyński, K. Rachlewicz, T. Głowiak, *Angew. Chem.* **1994**, *106*, 805; *Angew. Chem. Int. Ed. Engl.* **1994**, *33*, 779.
- [2] H. Furuta, T. Asano, T. Ogawa, *J. Am. Chem. Soc.* **1994**, *116*, 767.
- [3] P. J. Chmielewski, L. Latos-Grażyński, *J. Chem. Soc. Perkin Trans. 2* **1995**, 503.
- [4] T. D. Lash, D. T. Richter, C. M. Shiner, *J. Org. Chem.* **1999**, *64*, 7973.
- [5] Z. Xiao, B. O. Patrick, D. Dolphin, *Chem. Commun.* **2002**, 1816.
- [6] I. Schmidt, P. J. Chmielewski, Z. Ciunik, *J. Org. Chem.* **2002**, *67*, 8917.
- [7] P. J. Chmielewski, L. Latos-Grażyński, T. Głowiak, *J. Am. Chem. Soc.* **1996**, *118*, 5690.
- [8] P. J. Chmielewski, L. Latos-Grażyński, *Inorg. Chem.* **2000**, *39*, 5639.
- [9] P. J. Chmielewski, L. Latos-Grażyński, *Inorg. Chem.* **1997**, *36*, 840.
- [10] P. J. Chmielewski, L. Latos-Grażyński, I. Schmidt, *Inorg. Chem.* **2000**, *39*, 5475.
- [11] H. Furuta, N. Kubo, H. Maeda, T. Ishizuka, A. Osuka, H. Nanami, T. Ogawa, *Inorg. Chem.* **2000**, *39*, 5424.
- [12] T. Ogawa, H. Furuta, M. Takahashi, A. Morino, H. Uno, *J. Organomet. Chem.* **2000**, *611*, 551–557.
- [13] H. Furuta, T. Ogawa, Y. Uwatoko, K. Araki, *Inorg. Chem.* **1999**, *38*, 2676.
- [14] J. D. Harvey, C. J. Ziegler, *Chem. Commun.* **2002**, 1942.
- [15] D. S. Bohle, W.-C. Chen, C.-H. Hung, *Inorg. Chem.* **2002**, *41*, 3334.
- [16] H. Furuta, T. Ishizuka, A. Osuka, *J. Am. Chem. Soc.* **2002**, *124*, 5622.
- [17] W.-C. Chen, C.-H. Hung, *Inorg. Chem.* **2001**, *40*, 5070.
- [18] C.-H. Hung, W.-C. Chen, G.-H. Lee, S.-M. Peng, *Chem. Commun.* **2002**, 1516.
- [19] A. Srinivasan, H. Furuta, A. Osuka, *Chem. Commun.* **2001**, 1666.
- [20] H. Furuta, H. Maeda, A. Osuka, *Chem. Commun.* **2002**, 1795.
- [21] L. Latos-Grażyński, in *The Porphyrin Handbook*, Vol. 2 (Eds.: K. M. Kadish, K. M. Smith, R. Guilard), Academic Press, New York, **2000**, pp. 361–416.
- [22] M. Stępień, L. Latos-Grażyński, *Chem. Eur. J.* **2001**, *7*, 5113.
- [23] M. Stępień, L. Latos-Grażyński, T. D. Lash, L. Sztterenber, *Inorg. Chem.* **2001**, *40*, 6892.
- [24] M. Stępień, L. Latos-Grażyński, *J. Am. Chem. Soc.* **2002**, *124*, 3838.
- [25] S. Venkatraman, V. G. Anand, S. K. Pushpan, J. Sankar, T. K. Chandrashekar, *Chem. Commun.* **2002**, 462.
- [26] K. Berlin, E. Breitmaier, *Angew. Chem.* **1994**, *106*, 1356; *Angew. Chem. Int. Ed. Engl.* **1994**, *33*, 1246.
- [27] T. D. Lash, *Angew. Chem.* **1995**, *107*, 2703; *Angew. Chem. Int. Ed. Engl.* **1995**, *34*, 2533.
- [28] S. R. Graham, G. M. Ferrence, T. D. Lash, *Chem. Commun.* **2002**, 894.
- [29] M. A. Muckey, L. F. Szczepura, G. M. Ferrence, T. D. Lash, *Inorg. Chem.* **2002**, *41*, 4840.
- [30] N. Sprutta, L. Latos-Grażyński, *Tetrahedron Lett.* **1999**, *40*, 8457.
- [31] L. Sztterenber, N. Sprutta, L. Latos-Grażyński, *J. Inclusion Phenom.* **2001**, *41*, 209.
- [32] G. C. M. Lee, J. M. Holmes, D. A. Harcourt, M. E. Garst, *J. Org. Chem.* **1992**, *57*, 3126.
- [33] A. Ulman, J. Manassen, *J. Am. Chem. Soc.* **1975**, *97*, 6540.
- [34] I. Schmidt, P. J. Chmielewski, *Tetrahedron Lett.* **2001**, *42*, 1151.
- [35] V. Galasso, L. Klasinic, A. Sabljic, N. Trinajstic, G. C. Pappalardo, W. J. Steglich, *J. Chem. Soc. Perkin Trans. 2* **1981**, 127.
- [36] E. Orti, J. Sanchez-Marin, M. Merchan, F. Tomas, *J. Phys. Chem.* **1987**, *91*, 545.
- [37] D. R. Cullen, E. F. Meyer, Jr., *J. Am. Chem. Soc.* **1974**, *96*, 2095.
- [38] D. M. Grove, G. van Koten, H. J. C. Ubbels, R. Zoet, A. L. Spek, *Organometallics* **1984**, *3*, 1003.
- [39] P. W. Jolly, in *Comprehensive Organometallic Chemistry*, Vol. 6 (Eds.: G. Wilkinson, F. G. A. Stone, E. W. Abel), Oxford, **1984**, p. 37.
- [40] R. Forume, *Acta Crystallogr. Sect. B: Struct. Sci.* **1972**, *28*, 2984.
- [41] E. Vogel, J. Dörr, A. Herrmann, J. Lex, H. Schmickler, P. Walgenbach, J.-P. Gisselbrecht, M. Gross, *Angew. Chem.* **1993**, *105*, 1670; *Angew. Chem. Int. Ed. Engl.* **1993**, *32*, 1600.
- [42] E. Vogel, M. Sicken, P. Röhrig, H. Schmickler, J. Lex, O. Ermer, *Angew. Chem.* **1988**, *100*, 450; *Angew. Chem. Int. Ed. Engl.* **1988**, *27*, 411.
- [43] M. Pawlicki, L. Latos-Grażyński, L. Sztterenber, *J. Org. Chem.* **2002**, *67*, 5644.
- [44] L. Latos-Grażyński, J. J. Johnson, S. Attar, M. M. Olmstead, A. L. Balch, *Inorg. Chem.* **1998**, *37*, 4493.
- [45] H. Furuta, H. Maeda, A. Osuka, *J. Am. Chem. Soc.* **2000**, *122*, 803.
- [46] A. R. Karitzky, A. F. Pozharski, *Handbook of Heterocyclic Chemistry*, Pergamon, Amsterdam, **2000**.
- [47] 5-Anisol-dipyromethene has been isolated in the course of the preparation of an oxocarbaporphyrin in less than 1% yield. Once identified it could be readily detected in other syntheses leading to heteroporphyrins. ¹H NMR (CDCl₃): δ = 7.63 (s, 2H), 7.43 (d, 2H, ³J = 8.4 Hz), 6.96 (d, 2H, ³J = 8.4 Hz), 6.64 (d, 2H, ³J = 3.8 Hz), 6.39 (dd, 2H, ³J = 4.2, ⁴J = 1.5 Hz), 3.87 (s, 3H) ppm; ¹³C NMR (CDCl₃): δ = 160.4, 143.2 (5'), 142.2, 140.7 (2'), 132.4, 129.7, 128.7 (3'), 117.3 (4'), 113.0, 55.2 ppm; HRMS: *m/z*: calcd for C₁₆H₁₅N₂O₁ [M+H]⁺: 250.1184; found: 251.1179.
- [48] M. I. Bruce, P. Hinterding, P. J. Low, B. W. Skelton, A. H. White, *J. Chem. Soc. Dalton Trans.* **1998**, 467.
- [49] A. Thompson, D. Dolphin, *J. Org. Chem.* **2000**, *65*, 7870.
- [50] G. M. Sheldrick, *SHELXL97, program for crystal structure refinement*, University of Göttingen, **1997**.
- [51] G. M. Sheldrick, *SHELXS97, program for solution of crystal structures*, University of Göttingen, **1997**.

Received: March 4, 2003 [F4995]